The Null Flux Qubit

Raina J. Olsen
QSpice Labs Inc., 129 Mount Hope St., Kitchener, ON N2G 2J6, Canada

We discuss a superconducting flux qubit whose sensitivity to low frequency flux noise is greatly decreased through use of a null flux geometry.

Consider the two closed curves shown in Figure 1(a), which lie in the x, y plane with the x axis aligned with the longest dimension of the curve. These curves look fairly similar to one another when viewed from the top. Each has a pinched shape that splits the region of space within the curve into two loops, which we refer to as loops A and B. But there is one key difference between the two curves: the top curve has been twisted into a 'figure 8' shape, while the bottom curve remains flat and two-dimensional. When this 'figure 8' shape is symmetric and formed of conductive wire, it is an example of a null flux loop.

Null flux loops are so named because a current in the wire produces zero net flux. The arrows indicating current direction on the null flux loop in Fig. 1(a) show a clockwise current around loop A, which sets up a flux into the page, while the current is counter-clockwise around loop B, and so sets up a flux out of the page. As long as loops A and B are identical in shape and size, the flux through loop A exactly cancels the flux through loop B. In contrast, for the flat geometry the current is clockwise around both loops, so the net flux is non-zero.

Null flux systems are part of the guidance system of some Maglev (magnetic levitation) train systems, which were developed and used widely over the past century and currently still operate in Japan and South Korea. Null flux loops are used for stabilization in several different arrangements; one is to keep the train vertically aligned at a steady level above the track. In this arrangement, the loops are aligned vertically along the track, with the crossing between loops A and B positioned at the level that the train should stay in. A strong permanent magnet is in the side of the train at the same level. When the magnet in the train is stable at the same level as the crossing in the loop, an equal flux is set up through loops A and B.

Vertical motion of the permanent magnet will always have an opposite effect on the flux through the two loops (the flux through one loop increasing and the other decreasing). But because the two loops have opposite circulations, both induced currents will be in the same direction and the net energy of the system will increase and so oppose the vertical motion of the train. In contrast, horizontal motion of the permanent magnet will have the same effect on the flux through the two loops, with the induced currents tending to cancel. Therefore, the null flux loop has no impact on the horizontal motion of the train.

Now let us make a flux qubit out of the null flux loop by inserting a Josephson junction and derive the circuit

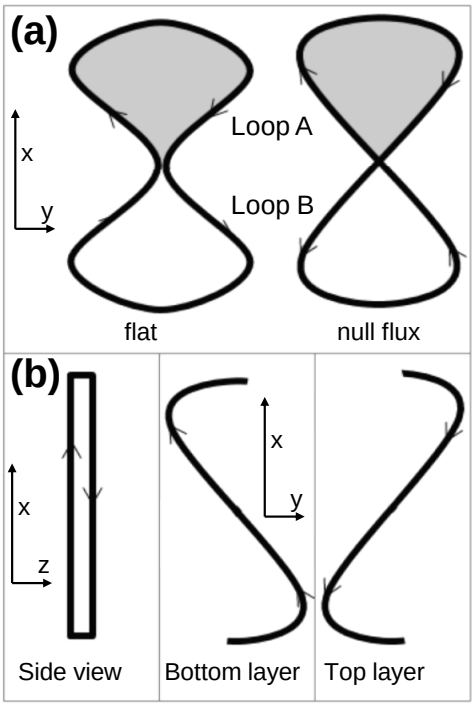

FIG. 1. (a) Comparison of two closed curves with different geometries. Both curves form two loops; A and B. The null flux curve is twisted into a three-dimensional 'figure 8' geometry, while the flat curve is two-dimensional. (b) Detail of one possible way to draw the null flux geometry in three-dimensional space.

behavior. We might expect to see the same functionality as in the train system - any external field that creates the same flux in loops A and B (be it a noise process or a control field) should not affect the energy levels, while any external field that creates an opposite flux in loops A and B should change the energy levels. For comparison, we will also derive the equations for the flat geometry.

Figure 2 shows the lumped element circuit if we place the Josephson junction in one side of the wire curve at the place where the two sides of the curve have their closest approach. The inductances in the circuit arise from the self inductance of loops A and B, while the capacitances arise from the close approach of the wires. The same circuit can be used for both the null flux geometry and the flat geometry. The only difference is in the directions of the loop fluxes, Φ_A, Φ_B, Φ_C, which we must carefully define for the following discussion.

For the flat geometry, both the circuit shown in Fig. 2

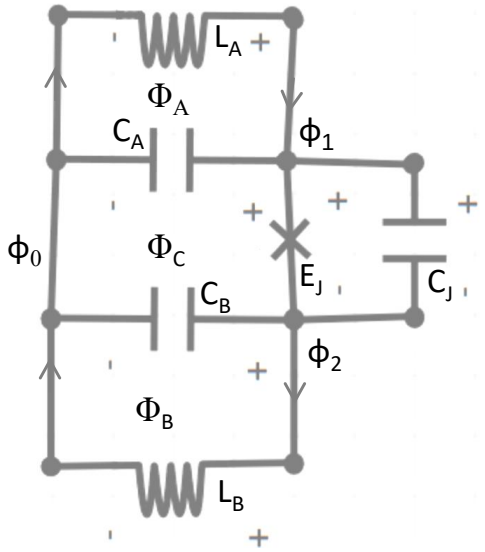

FIG. 2. The lumped element circuit corresponding to a wire shaped like either of the curves in Fig. 1(a), with a Josephson junction placed exactly between loops A and B.

	null flux geometry	flat geometry
loop A	$\hat{\phi}_{CA} - \hat{\phi}_{LA} = \Phi_A$	$\hat{\phi}_{CA} - \hat{\phi}_{LA} = \Phi_A$
loop B	$\hat{\phi}_{CB} - \hat{\phi}_{LB} = \Phi_B$	$\hat{\phi}_{CB} - \hat{\phi}_{LB} = -\Phi_B$
loop C	$\hat{\phi}_J + \hat{\phi}_{CB} - \hat{\phi}_{CA} = \Phi_C$	$\hat{\phi}_J + \hat{\phi}_{CB} - \hat{\phi}_{CA} = \Phi_C$
$\hat{\phi}_{LA}$	$\hat{\phi}_1 - \hat{\phi}_0$ $= \hat{\phi}_y$	$\hat{\phi}_1 - \hat{\phi}_0$ $= \hat{\phi}_y$
$\hat{\phi}_{LB}$	$\hat{\phi}_2 - \hat{\phi}_0$ $= \hat{\phi}_y - \hat{\phi}_x$	$\hat{\phi}_2 - \hat{\phi}_0$ $= \hat{\phi}_y - \hat{\phi}_x$
$\hat{\phi}_J$	$\hat{\phi}_1 - \hat{\phi}_2 + \Phi_A - \Phi_B + \Phi_C$ $= \hat{\phi}_x + \Phi_A - \Phi_B + \Phi_C$	$\hat{\phi}_1 - \hat{\phi}_2 + \Phi_A + \Phi_B + \Phi_C$ $= \hat{\phi}_x + \Phi_A + \Phi_B + \Phi_C$
$\hat{\phi}_{CA}$	$\hat{\phi}_1 - \hat{\phi}_0 + \Phi_A$ $= \hat{\phi}_y + \Phi_A$	$\hat{\phi}_1 - \hat{\phi}_0 + \Phi_A$ $= \hat{\phi}_y + \Phi_A$
$\hat{\phi}_{CB}$	$\hat{\phi}_2 - \hat{\phi}_0 + \Phi_B$ $= \hat{\phi}_y - \hat{\phi}_x + \Phi_B$	$\hat{\phi}_2 - \hat{\phi}_0 - \Phi_B$ $= \hat{\phi}_y - \hat{\phi}_x - \Phi_B$

TABLE I. Kirchhoff's voltage law equations and a corresponding set of branch equations for both loop geometries.

and the loop geometry shown in Fig. 1(a) lie in the x, y plane. To make the discussion simpler when we discuss the effect of externally applied fluxes, we will define all loop fluxes to be pointing in the same direction; into the page, in the $-z$ direction.

For the null flux geometry, the circuit in Fig. 2 lies in the x, z plane, corresponding to the side view in Fig. 1(b). For simplicity, we will define both Φ_A and Φ_B as pointing in the $-z$ direction; into the page relative to the top view in Fig. 1(a). With these definitions, when viewed from the side, Φ_A and $-\Phi_B$ point into the page. Finally, we define Φ_C as pointing into the page when viewed from the side. Therefore relative to the flat geometry, Φ_B acquires a minus sign in the null flux geometry while the other loop fluxes have the same direction.

Kirchhoff's voltage law equations for each loop and a corresponding set of branch equations that fulfill Kirchhoff's law are shown in Table I. Based on these equations, we can write the potential energy function for each loop geometry,

$$V_{null} = E_{LA}\hat{\phi}_y^2 + E_{LB}(\hat{\phi}_y - \hat{\phi}_x)^2 + E_J[1 - \cos(\hat{\phi}_x + \Phi_A - \Phi_B + \Phi_C)], \quad (1)$$

$$V_{flat} = E_{LA}\hat{\phi}_y^2 + E_{LB}(\hat{\phi}_y - \hat{\phi}_x)^2 + E_J[1 - \cos(\hat{\phi}_x + \Phi_A + \Phi_B + \Phi_C)], \quad (2)$$

where all fluxes are in dimensionless units of the magnetic flux quantum Φ_0, $E_L = \Phi_0^2/2L$, and we have defined $\hat{\phi}_x = \hat{\phi}_1 - \hat{\phi}_2$ and $\hat{\phi}_y = \hat{\phi}_1 - \hat{\phi}_0$.

The potential energy for the flat geometry is quite similar to the well-known Hamiltonian for the flux qubit, except that the harmonic term is now two dimensional and the externally applied flux is written as a sum of fluxes applied through different sections of the loop. In contrast, the *difference* of the fluxes applied through different sections of the loop appears in the potential energy for the null flux geometry.

Figure 3 compares a one-dimensional slice of the potential energy function for each loop. For the purposes of discussion, we will assume that the height of the null flux loop in the z direction is quite small compared to its length and width, such that the area of loop C is much smaller than the areas of loop A and B and so Φ_C can safely be neglected. For each loop, the potential energy is shown for zero applied flux, at an operating point where the potential has two degenerate wells, and near the operating point with a flux fluctuation in loop B that is equal to the flux fluctuation in loop A.

The operating point used is $\Phi_A = \Phi_B = \pi/2$ for the flat geometry and $\Phi_A = -\Phi_B = \pi/2$ for the null flux geometry. A constant, externally applied flux that takes this latter form could be applied in several ways, such as by a single control line that passes over the 'tie' in the bowtie shape with an orientation perpendicular to the wires, or by two control lines with different current directions, each placed closer to one of the 'bows.'

For the flat geometry, at the operating point we see the same well-known degenerate double well structure of the flux qubit. In response to a fluctuation in both loops, one well decreases in energy while the other increases in energy, resulting in both relaxation and dephasing.

For the null flux geometry, there is the same double well structure at the operating point, but the potential energy does not change in response to a fluctuation in both loops, thus no off-diagonal element arises in response and there is no relaxation. The diagonal elements

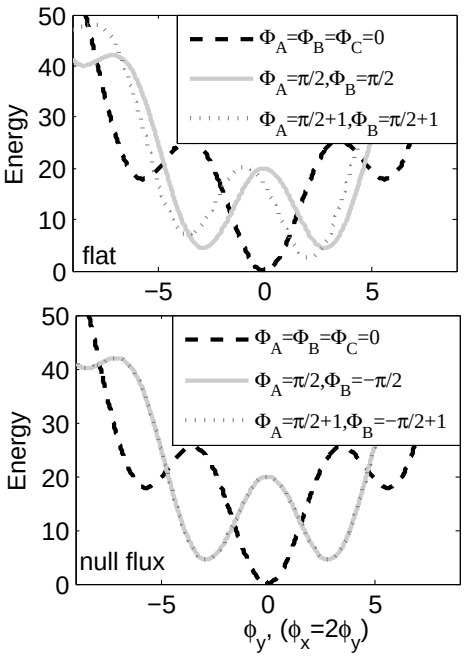

FIG. 3. The potential energy functions along the line $\hat{\phi}_x = 2\hat{\phi}_y$ for several different values of the applied flux and for each loop geometry.

will change because the derivative of the fluctuations appears in the kinetic term. Thus the null flux qubit will experience dephasing proportional to the amplitude and frequency of a fluctuation that has the same effect on both loops A and B.

In contrast, a fluctuation that has an opposite effect on the flux through two loops will cause relaxation and dephasing in the null flux qubit and only dephasing in the flat geometry flux qubit. Any real fluctuation will be a combination of these two types - one that has the same effect on the flux through the two loops, and one that has an opposite effect on the flux through the two loops.

Let us now consider in detail the way that interaction of the qubit with a classical electromagnetic plane wave is impacted by the null flux geometry. (Note that by using plane wave solutions, we are neglecting the impact of the superconducting loop or a ground plane on the electromagnetic wave.) Light with a half-wavelength, $\lambda/2$, that is similar to the distance between loops with different circulations will produce flux with different directions in each loop, thus strongly perturbing the energy levels of the qubit and causing relaxation. In contrast, light with a longer wavelength will produce flux with the same direction in each loop, thus having no net impact on the qubit energies. This means that the null flux qubit is *insensitive to low frequency photons*, with $\lambda \to 0$, a stunningly important result since decades of eperimental experience has found that flux noise is dominated by low frequency components.

In Figure 4, we show calculations of the net flux produced by light interacting with several different curve geometries. We assume that both the propagation direction and the E field lie within the x, y plane, as shown in Fig. 4(a), and that θ is the angle between the x axis and the direction of propagation. This makes the magnetic field,

$$\vec{B}_{\omega,\theta}(x,y,t) = A_{\omega,\theta} B_{\omega,\theta}(x,y,t)\hat{z}, \quad (3)$$

$$B_{\omega,\theta}(x,y,t) = \cos[\omega t - (x\cos\theta - y\sin\theta)]. \quad (4)$$

where ω is the frequency of the light and $A_{\omega,\theta}$ is an arbitrary normalization constant.

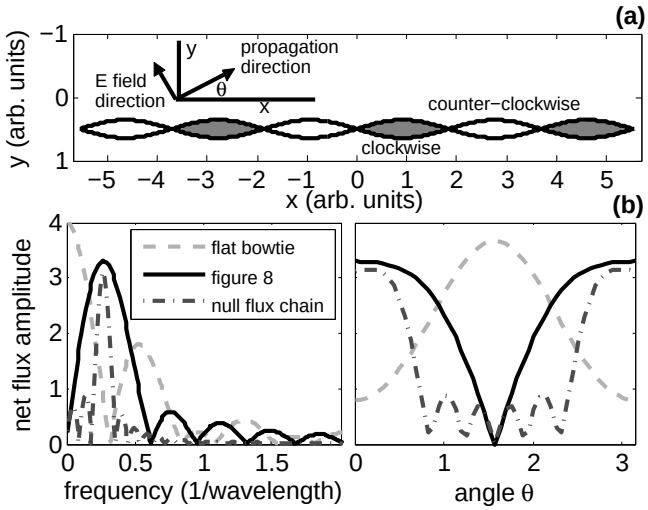

FIG. 4. (a) Depiction of a null flux chain composed of six loops (as opposed to the curves shown in Fig. 1, which are each composed of two loops). The chain is longer and narrower than the 'figure 8' loop, such that it has the same area. (b) Net flux through each curve as a function of ω (left, with $\theta = 0$) and θ (right, with $\omega = 0.37$). Results shown are in arbitrary units.

Each curve is composed of $i \geq 1$ loops, each with surface S_i and circulation $C_i = cw, ccw$. The flux through each of the loops is given by,

$$\vec{\Phi}_{i,\omega,\theta}(t) = \iint_{\vec{S}_i} \vec{B}_{\omega,\theta}(x,y) \cdot d\vec{S}. \quad (5)$$

The net flux through the loop is thus,

$$\vec{\Phi}_{\omega,\theta,j}(t) = \sum_{C_i=cw} a_{i,j}\vec{\Phi}_{i,\omega,\theta}(t) - \sum_{C_i=ccw} a_{i,j}\vec{\Phi}_{i,\omega,\theta}(t), \quad (6)$$

where $a_{i,j} = 0, 1$ is a binary vector associated with component j that depends on the definition of the circuit's spanning tree. These net fluxes will appear in the potential energy function corresponding to component j (as in Eq. 1). Taken together, the net fluxes are proportional to the impact of light at frequency ω on decoherence of a qubit with the curve geometry. The amplitude of the net flux, $\max(\Phi_{\omega,\theta}(t))$ with $a_{i,j} = 1$, is shown in Figure 4(b) as a function of both ω and θ.

It is clear to see the important difference between the flat geometry and the null flux 'figure 8' geometry in Figure 4. Light produces the largest net flux through the flat curve at $\omega \to 0$, but the net flux curve is most strongly affected by light at a higher frequency, which is inversely proportional to the distance between loops with opposite circulations. The frequency profiles are broad for both loops, but fall off at high frequency, as the wavelength becomes much smaller than the loop size. The profile in both frequency and angle may be narrowed through design of the null flux geometry, such as by increasing the number of loops from two, as depicted in Fig. 4(a).